Miniemulsion Polymerization of Styrene with Polymeric Costabilizers

Chorng-Shyan Chern, Chi-Han Lin

Department of Chemical Engineering, National Taiwan University of Science and Technology, 43 Keelung Road, Section 4, Taipei 106, Taiwan

ABSTRACT: The polymeric costabilizers poly(stearyl methacrylate-*co*-2-hydroxyethylmethacrylate) (PSH) and poly(lauryl methacrylate-*co*-2-hydroxyethylmethacrylate) (PLH), composed of a hydrophilic backbone and several hydrophobic alkyl (stearyl or lauryl) side chains, were prepared by the free-radical copolymerization of stearyl methacrylate (SMA) or lauryl methacrylate (LMA) with 2-hydroxyethylmethacrylate and evaluated in the miniemulsion polymerization of styrene (ST). For comparison, the reactive costabilizers SMA and LMA were also included in this work. The hydrophobicity of costabilizers in increasing order was PLH < PSH < LMA < SMA. Only a small amount of these comb-like copolymers was capable of pro-

ducing kinetically stable ST emulsion droplets. The more hydrophobic the costabilizer was, the more effective was the costabilizer in the retardation of Ostwald ripening. About 30–40% of the monomer droplets were successfully converted into latex particles during the polymerization. The degree of monomer droplet nucleation increased with increasing hydrophobicity of the costabilizer. The formation of particle nuclei in the continuous aqueous phase played a crucial role in the polymerization kinetics. © 2004 Wiley Periodicals, Inc. J Appl Polym Sci 92: 1961–1969, 2004

Key words: emulsion polymerization; colloids; particle nucleation

INTRODUCTION

In emulsion polymerization, the primary particle nucleation loci include the monomer-swollen micelles and the continuous aqueous phase.[1] Ugelstad et al.[2] showed that monomer droplets became the predominant nucleation loci when the size of these droplets was reduced to the submicron level (termed *miniemulsion polymerization*[3]). This was attributed to the very large droplet surface area available for the capture of free radicals generated in the aqueous phase. A low-molecular-weight hydrophobic compound, such as hexadecane or cetyl alcohol (CA), was required to impart adequate colloidal stability to the monomer droplets.[2,4,5]

Schork and coworkers[6–10] and Blythe et al.[11] demonstrated that incorporation of a small amount of polymeric costabilizer [e.g., polymethyl methacrylate, polystyrene (PS)] into monomer droplets retarded the diffusion of monomer molecules from small droplets to large ones (Ostwald ripening). This allowed nucleation in these kinetically stable droplets by the entry of radicals. El-Aasser and coworkers[12–17] observed enhanced droplet nucleation in the CA-containing styrene (ST) miniemulsion polymerization in the presence of predissolved PS in the monomer phase.[16,17]

In our previous study, the effectiveness of stearyl methacrylate (SMA) or lauryl methacrylate (LMA) as a reactive costabilizer for the stabilization of the ST miniemulsion polymerization was evaluated.[18,19] An extremely hydrophobic blue dye was adopted to study the particle nucleation mechanisms.[20] The water solubility of this dye was about 1 ppm,[21] that is, two orders of magnitude smaller than that of ST (~200 ppm). The amount of dye ultimately incorporated into latex particles was used to study the extent of monomer droplet nucleation because these dye molecules were incapable of diffusing from those droplets that had not been nucleated through the continuous aqueous phase and then into latex particles. It was shown that in addition to monomer droplet nucleation, the formation of particle nuclei in the aqueous phase (homogeneous nucleation) also played an important role in the polymerization kinetics. The less hydrophobic LMA [water solubility of LMA (1.38×10^{-8}) > SMA $(3.23 \times 10^{-9}$ mL/mL)[22]] was less effective in retarding Ostwald ripening, and therefore, the LMA-containing polymerization exhibited stronger homogeneous nucleation compared to the SMA counterpart.

It was shown that the reactive costabilizer SMA (or LMA) imparted adequate colloidal stability to ST miniemulsions.[18,19] After the nucleation of miniemulsion droplets, the copolymer of ST and SMA (or LMA) formed therein, and the residual SMA (or LMA) played a more important role in the stabilization of latex particles during the early stage of polymeriza-

Correspondence to: C.-S. Chern (chern@ch.ntust.edu.tw).

tion. Thus, it is important to study the effectiveness of polymeric costabilizers containing monomeric units of SMA (or LMA) to gain a better understanding of miniemulsion polymerization with SMA (or LMA) as the reactive costabilizer. The objective of this preliminary study was to carry out the free-radical copolymerization of SMA (or LMA) and 2-hydroxyethyl methacrylate (HEMA) and then to evaluate the performance of these novel polymeric costabilizers composed of a hydrophilic backbone and several hydrophobic alkyl (stearyl or lauryl) side chains in the ST miniemulsion polymerization. It was interesting to study the effects of the reduced hydrophobicity and increased molecular weight associated with these polymeric costabilizers. This might have provided a conservative estimation of the contribution of the more hydrophobic copolymer of ST and SMA (or LMA) in the stabilization of the ST miniemulsion polymerization, provided that the hydrophobicity of polymeric costabilizer was the key parameter. Furthermore, the results obtained from this study might help polymer chemists design more effective comb-like polymeric costabilizers. For comparison, SMA- and LMA-containing polymerizations were also included in this study.

EXPERIMENTAL

Materials

The chemicals used in this work included ST (Taiwan Styrene Co., Kaohsiung, Taiwan), HEMA (Aldrich, Shanghai, China; 97%), SMA (Mitsubishi Rayon, Tokyo, Japan), LMA (Aldrich), lauryl mercaptan (Aldrich), 2,2′-azobisisobutyronitrile (AIBN; Showa, Osaka, Japan), sodium persulfate (SPS) (Riedel-de Haen, Hanover, Germany), sodium lauryl sulfate (SLS; J. T. Baker, Phillipsburg, NJ; 99%), sodium bicarbonate (Riedel-de Haen), anhydrous magnesium sulfate (Yakuri Chemicals, Osaka, Japan), a water-insoluble blue dye (Blue 70; its molecular structure can be found in ref. [23]; Shenq-Fong Fine Chemical Ltd., China), d-chloroform (Isotec, Miamisburg, OH), tetrahydrofuran (THF; Merck, Germany), potassium hydrogenphthalate (Hayashi, Osaka, Japan), and deionized water (Barnsted, Iowa; Nanopure Ultrapure Water System, specific conductance < 0.057 μS/cm). SMA (or LMA) and AIBN were purified by recrystallization from ethanol and methanol, respectively. ST was distilled at 40°C under reduced pressure before use. All other chemicals were used as received.

Synthesis of polymeric costabilizers

The polymeric costabilizer poly(stearyl methacrylate-co-2-hydroxyethylmethacrylate) [PSH; or poly(lauryl methacrylate-co-2-hydroxyethylmethacrylate) (PLH)] was prepared by the copolymerization of HEMA and
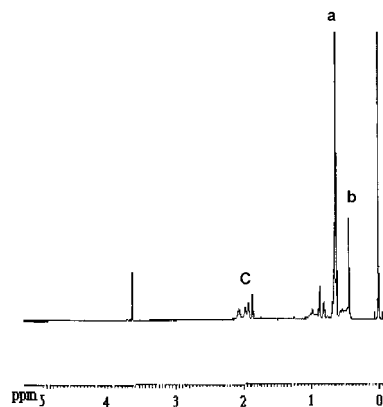

Figure 1 H-NMR spectrum of the polymeric costabilizer PSH.

SMA (or LMA) in acetone/methanol (90/10% w/w) with AIBN and lauryl mercaptan as the initiator and chain-transfer agent, respectively. The molar ratio of HEMA to SMA (or LMA) was 65 : 35, and the levels of lauryl mercaptan and AIBN were 8 and 10% on the basis of the total monomer weight, respectively. Batch polymerization was carried out in a 250-mL reactor equipped with a four-bladed fan turbine agitator, a thermometer, and a reflux condenser. The reaction mixture was purged with N_2 for 15 min while the temperature was brought to 60°C. This was followed by the addition of AIBN to initiate the polymerization over 8 h. The theoretical total solids content of the product was 12.5%. The volume of the resultant polymer solution was reduced to 30% by a rotary evaporator before the polymer product PSH (or PLH) was precipitated from ethanol (or n-hexane) three times and then dried in vacuo.

The compositions of the polymeric costabilizers were determined by ^{1}H-NMR (Varian Gemin 2000, 500 MHz; Palo Alto, CA) at ambient temperature in CDCl$_3$ containing 0.05% (v/v) of tetramethylsilane as the internal standard. The ^{1}H-NMR spectra, obtained from SMA, LMA, and HEMA, were used to facilitate the structural identification. The molar ratio of SMA (or LMA) to HEMA of the polymeric costabilizer was obtained from the corresponding integrated areas of signals attributed to $-CH_2-C(CH_3)C(O)O-CH_2{}^c-(CH_2{}^c-(CH_2{}^a)_{n=15}-CH_3{}^b$ (a: δ = 1.26 ppm; b: δ = 0.90 ppm) of SMA (or LMA, n = 9) and $-CH_2-C(CH_3)C(O)O-CH_2{}^c-CH_2{}^c-OH$ (c: δ = 3.70–4.15 ppm) of HEMA (Fig. 1). The contribution of $-CH_2{}^c-CH_2{}^c$ (c: δ = 3.70–4.15 ppm) of SMA (or LMA) was taken into account in the determination of the HEMA content. The number-average molecular weight (M_n), weight-average molecular weight (M_w), and polydispersity index {PDI [molecular weight distribution (MWD)] = M_w/M_n} were determined by gel permeation chromatography (GPC) (Waters Styragel HR2, HR4, and HR6; Milford, MA). THF was used as the elution solvent, and PS standards (Polysciences) were used to construct the calibration curve.

Preparation and miniemulsion polymerization of ST

The homogenized emulsion was prepared by the dissolution of SLS in water and of the costabilizer and dye in ST, respectively. The oily and aqueous solutions were mixed with a mechanical agitator at 400 rpm for 10 min. The resultant emulsion was then homogenized by a Microfluidizer-110Y (Microfluidics, Newton, MA) operated at a 5000-psi outlet pressure for 10 passes. The shelf-life was monitored by the placement of 100 mL of the sample in a capped glass vial at 35°C.

Immediately after homogenization, the emulsion was charged into a 250-mL reactor equipped with a four-bladed fan turbine agitator, a thermometer, and a reflux condenser and was then purged with N_2 for 10 min while the temperature was brought to 80°C. The emulsion charge was composed of 40 g of H_2O, 2.66 mM $NaHCO_3$, 10 mM SLS, 3.5 mM costabilizer, 2.33 M ST, 0.24 mM dye, and 2.66 mM SPS, where all the molar concentrations were based on the aqueous phase. The concentration of polymeric costabilizer was defined as the number of moles of the monomeric unit of SMA (or LMA) in the copolymer per unit volume of water. The polymerization temperature was kept constant at 80°C. The theoretical solids content of the latex product was 20%.

Determination of the monomer droplet size (or latex particle size)

The average monomer droplet diameter immediately before the start of polymerization ($d_{m,i}$) and the average colloidal particle diameter during polymerization (d), were determined by dynamic light scattering (DLS; Otsuka Photal LPA 3000/3100, Osaka, Japan). The cumulant method was chosen for the measurement of the z-average hydrodynamic diameter of colloidal particles. The dilution water was saturated with SLS (critical micelle concentration = 8.2 mM[24]) and ST (1.92 mM[25]) to avoid the diffusion of SLS and ST from the monomer droplets (or monomer-swollen latex particles) into the aqueous phase. The reported data of $d_{m,i}$ and d represent the average of at least three measurements, and their errors were estimated to be 8% or less. The volume-average diameter (d_v), weight-average diameter (d_w), and PDI [PDI (PSD) = d_w/d_n] of the dried latex particles were determined by transmission electron microscopy (TEM; Jeol TEM-1200 EXII, Tokyo, Japan), where d_n is the number-average diameter. On the basis of the $d_{m,i}$ and d_v data, the number of monomer droplets per liter of water immediately before the start of polymerization ($N_{m,i}$) and the number of latex particles per liter of water at a certain monomer conversion (N_P) were calculated.

TABLE I
Some Physical Properties of the Polymeric Costabilizers

Costabilizer	PSH	PLH	SMA	LMA
M_n	5500	3600	339	254
PDI (MWD)	1.24	1.35		
SMA (or LMA)/HEMA molar ratio	1.43 : 1	0.78 : 1		
Number of SMA (or LMA) per chain	15.7	11.6		
μ (D mol$^{-3/2}$)	0.045	0.056	0.035	0.041

Characterization of the latex particles

The latex product was filtered through 40-mesh (0.42 mm) and 200-mesh (0.074 mm) screens in series to collect filterable solids. Scraps adhering to the agitator, thermometer, and reactor wall were also collected. The total solids content and conversion of ST (X) were determined gravimetrically. The ζ potential of latex particles was determined by a Zetamaster (Malvern, Worcestershire, UK). The sample, with a volume of 0.1 mL, was diluted with 39.9 mL of 0.05 mM potassium hydrogenphthalate buffer solution (pH 4). The reported ζ represents an average of 10 measurements. M_w of the emulsion polymer was obtained from GPC.

The following procedure, developed in ref. 20, was modified slightly to determine the dye content within latex particles. The sample was first coagulated by magnesium sulfate. Precipitated polymer particles were washed three times with an excess of methanol to completely remove those dye molecules that were not incorporated into particles during polymerization and that were located in the interstitial spaces between the coagulated particles. This was followed by three rinses of the precipitate by an excess of water. Approximate 0.5 g of dried polymer was then dissolved in 20 mL of THF for the determination of the dye content by the ultraviolet (UV) absorbance method (Shimadzu, UV-160A, Sydney, Australia). The extinction coefficient obtained from the calibration curve of the UV absorbance at 678 nm versus the dye concentration data was 7.313×10^4 mL cm^{-1} g^{-1}. The reported weight percentage of dye incorporated into latex particles (P_{dye}) represents the average of five measurements.

RESULTS AND DISCUSSION

Characterization of the polymeric costabilizers

Some physical properties of PSH and PLH are listed in Table I. On average, PSH (or PLH) had 16 monomeric units of SMA (or 12 monomeric units of LMA) per chain. The theoretical dipole moment on on the basis of unit volume [μ (D cm$^{-3/2}$)] was calculated with the following equation:[26]

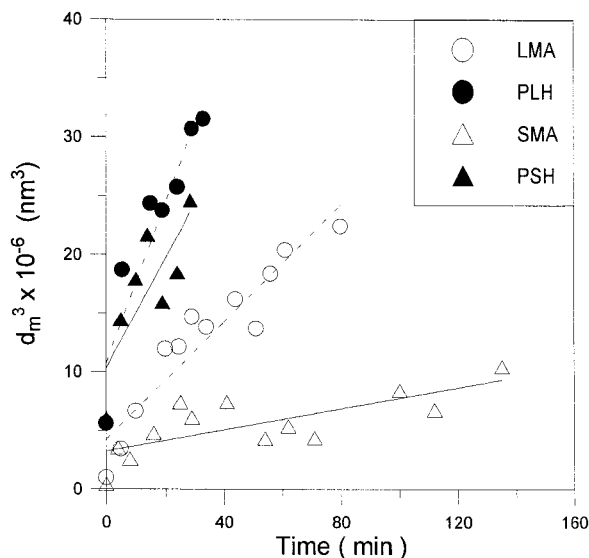$$\mu = [(P_{LL} - R_{LL})/(20.6V)]^{1/2} \qquad (1)$$

Figure 2 Average monomer droplet diameter (d_m) on aging at 35°C as a function of time for homogenized ST emulsions prepared by various costabilizers: [SLS] = 10 mM; costabilizer concentration = 3.5 mM; (▲) PSH, (●) PLH, (△) SMA, and (○) LMA.

where P_{LL} and R_{LL} are the molar dielectric polarization, and molar refraction, respectively, and V is the molar volume. The values of P_{LL}, R_{LL}, and V were obtained from ref. 26. The larger μ was, the more hydrophilic the costabilizer was. The hydrophobicity in increasing order was PLH < PSH < LMA < SMA. PSH was more hydrophobic than PLH because the water solubility of SMA was much lower, and furthermore, more monomeric units of SMA could be incorporated into the copolymer, as shown by the SMA (or LMA)/HEMA molar ratio, as shown in Table I.

Colloidal stability of the homogenized ST emulsions

According to the extended Lifshitz–Slyozov–Wagner theory, the rate of Ostwald ripening [$d(d_m^3)/dt$] can be predicted by the following equation:[27]

$$d(d_m^3)/dt = 64\sigma D_{c0}V_m C_{c0}(\infty)/(9RT\varphi_{c0}) \qquad (2)$$

where t is time, σ is the oil–water interfacial tension, D_{c0} is the molecular diffusivity of the costabilizer in water, V_m is the molar volume of the substance in the droplet, $C_{c0}(\infty)$ is the solubility of the bulk costabilizer in water, R is the gas constant, T is the absolute temperature, and φ_{c0} is the volume fraction of costabilizer in the droplet. Figure 2 shows the d_m^3 versus t data for homogenized ST emulsions stabilized by 10 mM SLS and 3.5 mM costabilizer at 35°C. To rigorously evaluate the performance of polymeric costabilizer, we used a costabilizer concentration of 3.5 mM, which was about one order of magnitude lower than those reported in the literature. The Ostwald ripening rate was determined by the least squares best-fitted slope of the d_m^3 versus t data (Table II). Although the experimental data were somewhat scattered, as shown by the values of the coefficient of determination in Table II, $d(d_m^3)/dt$ in decreasing order was PLH > PSH > LMA > SMA. This trend was consistent with the hydrophobicity of costabilizer. The larger μ was, the less effective the costabilizer was in retarding Ostwald ripening [i.e., $d(d_m^3)/dt$ increased linearly with increasing $C_{c0}(\infty)$], as shown in Figure 3. Another contributing factor to the inferior performance of polymeric costabilizer PSH (or PLH) was its weaker capability of swelling monomer droplets compared to the low-molecular-weight counterpart SMA (or LMA), as illustrated by equilibrium swelling thermodynamics.[28]

TABLE II
Ostwald Ripening Rate Data and Results Obtained from the ST Miniemulsion Polymerizations Stabilized by Various Costabilizers

Costabilizer	PSH	PLH	SMA	LMA
$d(d_m^3)/dt \times 10^5$ (nm^3/min)	4.6 (0.6471)[a]	6.7 (0.8698)[a]	0.45 (0.5552)[a]	1.5 (0.8870)[a]
$d_{m,i}$ (nm)[b]	332	311	252	271
d_v (nm)[c]	64	52	86	82
PDI (PSD)[c]	1.05	1.07	1.01	1.02
$N_{m,i} \times 10^{-16}$ (L^{-1})[b]	1.5	1.8	3.0	2.7
$N_p \times 10^{-17}$ (L^{-1})[c]	16.4	25.5	7.1	6.2
$R_p \times 10^2$ (mol L^{-1} min^{-1})	9.1	15.0	4.9	4.9
$n[M]_p$ (M)	1.2	1.1	1.5	1.7
$P_{dye,max}$ (%)	34	41	34	31
$N_{m,i}P_{dye,max} \times 10^{-15}$	5.1	7.4	10.2	8.4
$(N_{m,i}P_{dye,max}/N_p) \times 10^3$	3.1	2.9	14.4	13.5
Total scraps (%)	0.07	0.08	0.05	0.04

[a] The numeric values in the parentheses are the coefficients of determination.
[b] Determined at the very beginning of polymerization.
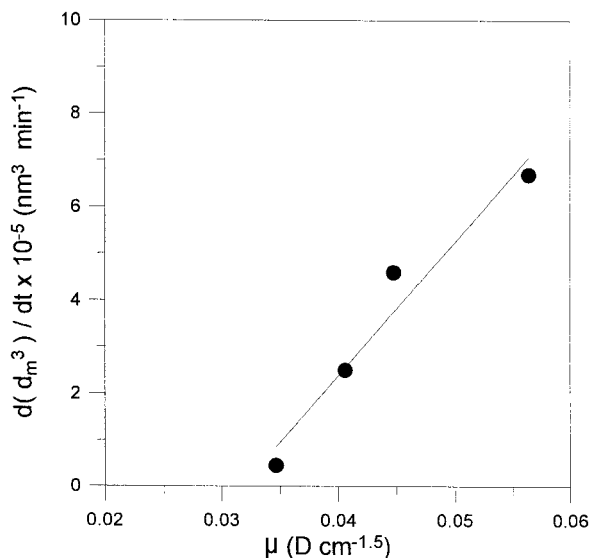[c] Determined at the end of polymerization.

Figure 3 $d\,(d_m^3)/dt$ versus μ of the various costabilizers: [SLS] = 10 mM; costabilizer concentration = 3.5 mM: The coefficient of determination for the least squares best-fitted straight line was 0.9533.

Figure 5 X as a function of time for the ST miniemulsion polymerizations prepared by various costabilizers: [SLS] = 10 mM; costabilizer concentration = 3.5 mM; (▲) PSH, (●) PLH, (△, ▲) SMA, and (○, ●) LMA.

The creaming rate data are shown in Figure 4, where the ordinate represents the position of the creaming line from the bottom of the sample. The creaming rate in decreasing order was PLH ≈ PSH > LMA > SMA. Creaming could be described by the Stokes terminal velocity equation, and its rate was proportional to d_m^{2}.[29] The creaming rate data reflected the degree of Ostwald ripening; emulsions stabilized by PLH or PSH experienced stronger Ostwald ripen-
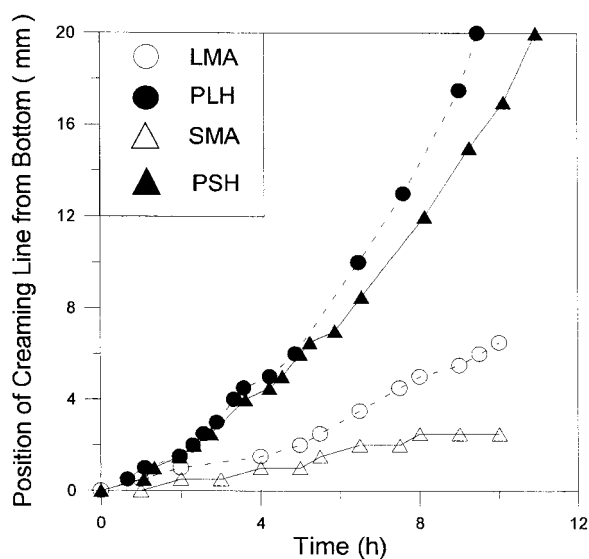

Figure 4 Position of creaming line from the bottom of the sample on aging at 35°C as a function of time for homogenized ST emulsions prepared by the various costabilizers: [SLS] = 10 mM; costabilizer concentration = 3.5 mM; (▲) PSH, (●) PLH, (△) SMA, and (○) LMA.
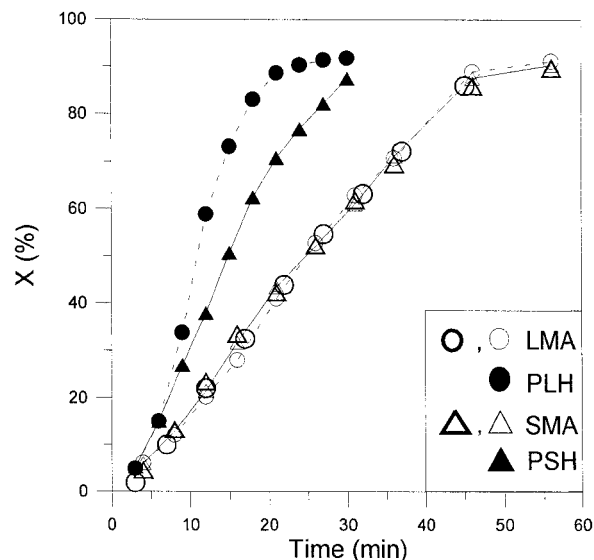
ing, thereby leading to a larger d_m. This resulted in a faster creaming rate in comparison with those emulsions containing LMA or SMA.

Miniemulsion polymerization of ST

The X versus t profiles for the ST miniemulsion polymerizations stabilized by 10 mM SLS and 3.5 mM costabilizer are shown in Figure 5. Both runs, with SMA and LMA, were carried out twice, and the reproducibility of the kinetic data was satisfactory. Some experimental results are also included in Table II. All of the polymerizations exhibited very good colloidal stability, as shown by the very low total scraps (Table II).

Although the rate of Ostwald ripening of the emulsion with LMA was about three times that of the emulsion with SMA (Table I), the SMA- and LMA-containing runs showed comparable rates of polymerization [$R_p = [M]_0 dX/dt$, where $[M]_0$ is the initial concentration of the monomer on the basis of total water (2.33M) and dX/dt can be obtained from the least squares best-fitted slope of the linear portion of the X versus t curve; Fig. 5 and Table II]. Other experimental data, such as d_v, PDI (PSD), N_p, and the maximum weight percentage of dye incorporated into latex particles ($P_{dye,max}$), also suggested that the SMA- and LMA-containing polymerizations showed very similar kinetics (Table II). With the knowledge of R_p, the propagation rate constant [$k_p = 4.27 \times 10^7 \exp(-32{,}510/RT)$ L mol^{-1} s^{-1}[30]], and N_p, the product of the average number of radicals per particle (n) and the concentration of monomer in the particle during
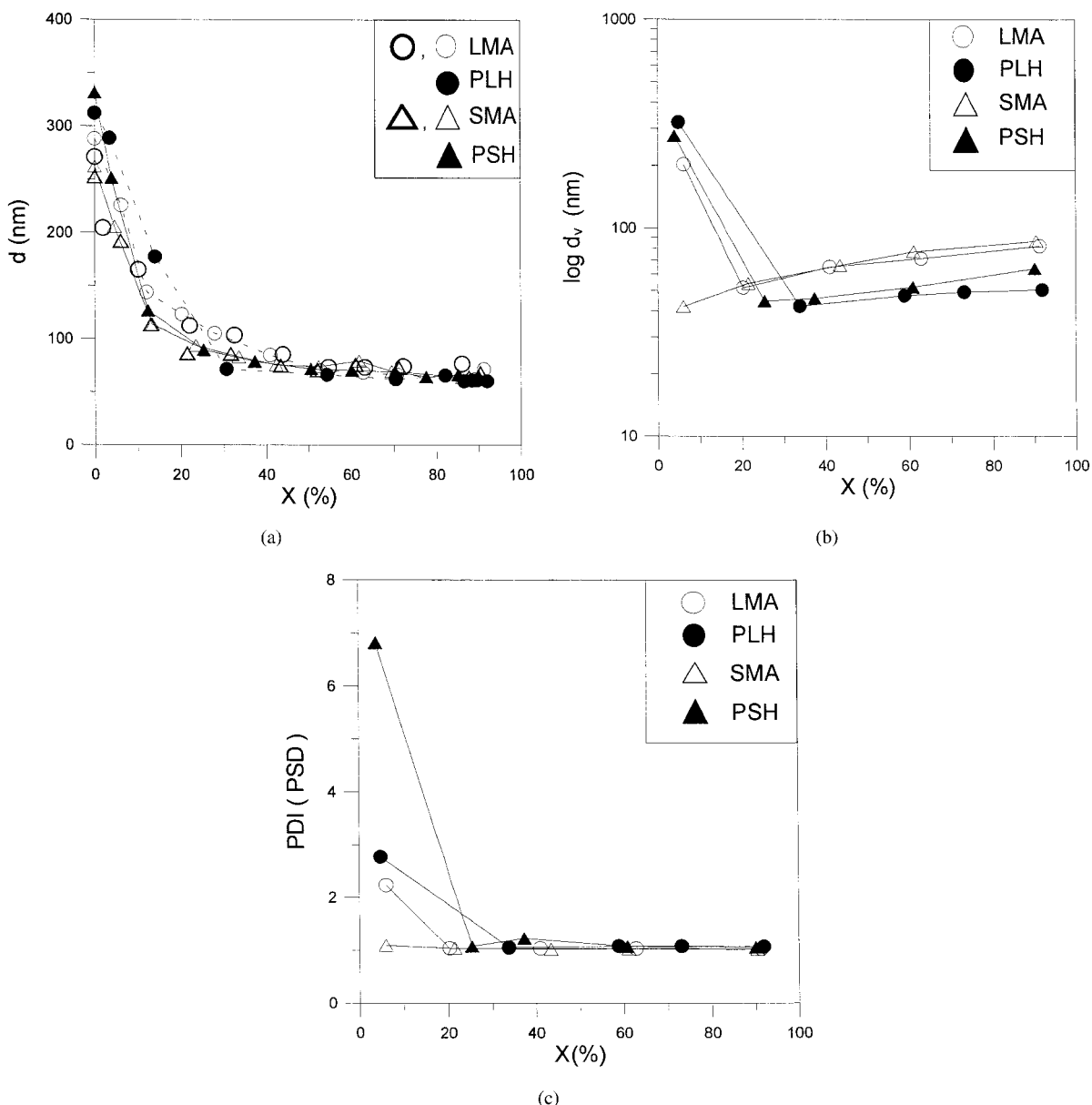
(a)

(b)

(c)

Figure 6 (a) d of colloidal particles determined by DLS, (b) d_v of dried polymer particles determined by TEM, and (c) PDI (PSD) of dried polymer particles of latex samples taken during polymerization versus conversion data in the ST miniemulsion polymerizations with different costabilizers: [SLS] = 10 mM; costabilizer concentration = 3.5 mM; (▲) PSH, (●) PLH, (△, ◬) SMA, and (○, ◯) LMA.

the constant R_p period ($[M]_p$) can be estimated by the following equation:

$$R_p = k_p[M]_p(nN_p/N_A) \tag{3}$$

where N_A is Avogadro's number. The SMA- and LMA-containing polymerizations had a comparable number (N_p) and size (d_v and PDI (PSD)] of reaction loci and $[M]_p$. Furthermore, these two polymerizations were expected to have similar values of n because n is primarily governed by the absorption, desorption, and termination of radicals, which are closely related to d_v

and $[M]_p$. All of these factors may have thus contributed to the same R_p in the SMA- and LMA-containing polymerizations.

Figure 6 shows the average colloidal particle diameter determined by DLS (d) and d_v and PDI (PSD) of dried particles determined by TEM versus X data. For both the SMA- and LMA-containing polymerizations, d first decreased rapidly, from about 260 to 100 nm, and then leveled off. The rapidly decreased d with X could be attributed to the formation of particle nuclei in the aqueous phase or micelles.[18,20] Chang et al.[31] showed that micelles did not form until the SLS con-
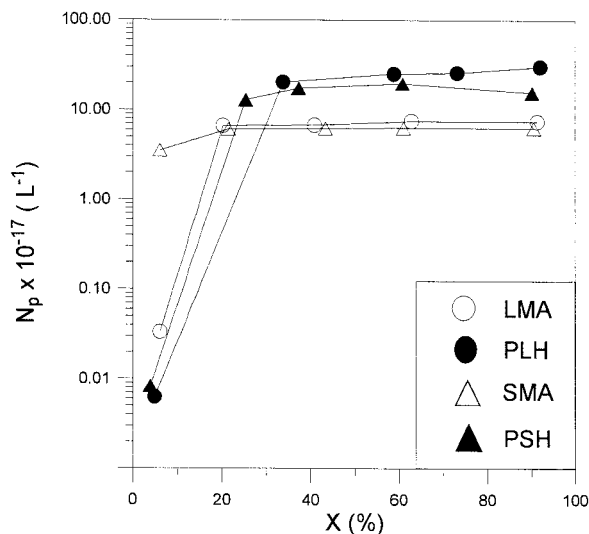
Figure 7 N_p as a function of X for the ST miniemulsion polymerizations prepared by various costabilizers: [SLS] = 10 mM; costabilizer concentration = 3.5 mM; (▲) PSH, (●) PLH, (△) SMA, and (○) LMA.

centration ([SLS]) exceeded 33 mM for ST miniemulsions. Thus, micellar nucleation could be ruled out because the [SLS] used in this work was only 10 mM. If we assumed that no coalescence among monomer droplets occurred during polymerization, the maximum number of particles generated by monomer droplet nucleation was $N_{m,i}P_{dye,max} = 1.0 \times 10^{16}$ and 8.4×10^{15} L^{-1} for the SMA- and LMA-containing polymerizations respectively. This suggested that although a significant fraction (~ 30%) of monomer droplets could be transformed into latex particles, homogeneous nucleation played an important role in the polymerization kinetics. This was because the population of latex particles originating from monomer droplet nucleation only represented a small fraction of the total number of latex particles produced (see the N_p data in Table II).

It was shown that SMA was more effective in retarding Ostwald ripening, and therefore, monomer droplet nucleation played a more important role in the ST polymerization with 5 mM SLS and 20 mM SMA compared to the LMA counterpart. Thus, the SMA- and LMA-containing polymerizations showed quite different reaction kinetics.[18,20] However, the SMA or LMA concentration (3.5 mM) used in the present study was so low that the different reaction kinetics could be detected only at the very beginning of polymerization [see the d_v and PDI (PSD) data in Figs. 6(b) and 6(c) respectively, and the N_p data in Fig. 7]. At very low X, the run with SMA resulted in a smaller d_v (i.e., larger N_p) in comparison with the LMA counterpart (Figs. 5 and 7). Nevertheless, the influence of costabilizers with different hydrophobicities did not persist long enough because of the very low costabilizer concentration used to stabilize monomer drop-

lets. Immediately after a significant population of latex particles generated via homogeneous nucleation built up, d_v, PDI (PSD), N_p, and, consequently, the polymerization kinetics were no longer distinguishable in the SMA- and LMA-containing runs.

The results obtained from polymerizations with 10 mM SLS and 3.5 mM PSH (or PLH) are shown in Figures 5–7 and Table II. R_p in decreasing order was PLH > PSH > SMA ≈ LMA (see Fig. 5 and the R_p data in Table II). This trend was closely related to the number of reaction loci (i.e., N_p) available for the polymerization to take place. The smaller d_v (i.e., the larger N_p) was, the faster R_p was [see Figs. 6(b) and 7 and the N_p data in Table II]. The more hydrophilic PLH (or PSH) was less effective in stabilizing monomer droplets against Ostwald ripening, and therefore, larger monomer droplets were produced in comparison with the LMA (or SMA) counterpart, as shown by the $d_{m,i}$ data in Table II. Thus, the PLH- (or PSH)-containing polymerization had a smaller monomer droplet surface area available for capturing radicals to induce particle nucleation as compared to the LMA (or SMA) counterpart. Figure 6(a) shows that in comparison with the LMA (or SMA) counterpart, the extent of reduction in d during the early stage of the reaction was greater for the PLH- (or PSH-) containing polymerization as a result of the stronger Ostwald ripening effect (Fig. 2). It was then postulated that for the PLH- (or PSH-) containing polymerization, the formation of more particle nuclei in the aqueous phase was responsible for the faster R_p.

Figure 8 shows that P_{dye} first increased to a maximum ($P_{dye,max}$; Table II) around $X = 34-43\%$ and then
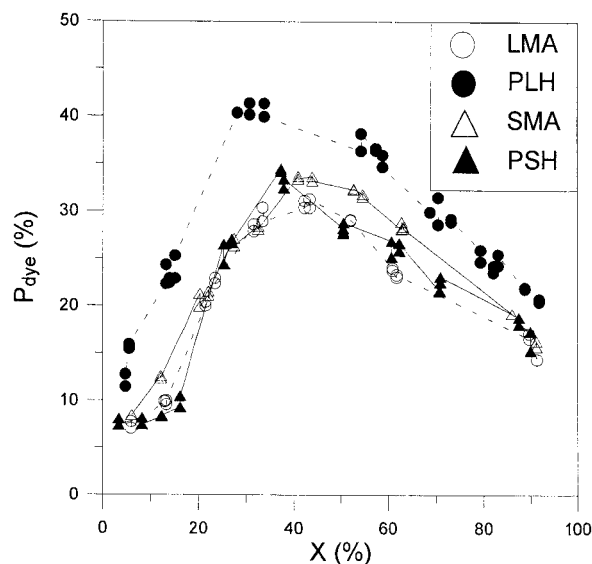

Figure 8 P_{dye} for latex samples taken at various levels of X in the ST miniemulsion polymerizations with different costabilizers: [SLS] = 10 mM; costabilizer concentration = 3.5 mM; (▲) PSH, (●) PLH, (△) SMA, and (○) LMA.

decreased toward the end of polymerization. The increased P_{dye} with X indicated that monomer droplet nucleation did not cease until 34–43% conversion was achieved. Beyond the point at which $P_{dye,max}$ occurred, the decreased P_{dye} with X was attributed to the diminished monomer droplet nucleation, the continuous formation of particle nuclei in the aqueous phase, and the polymerization inside the existing latex particles (i.e., the dilution of dye in the emulsion polymer). At a constant X, the run with the most hydrophilic PLH exhibited the largest P_{dye}. This implied that the fraction of monomer droplets that could be transformed into latex particles was the largest for the PLH-containing polymerization. Furthermore, polymerizations with PSH, SMA, and LMA showed comparable P_{dye} versus X profiles. The probability for radicals to enter monomer droplets (i.e., the amount of dye that could be incorporated into latex particles) increased with increasing total droplet surface area. At a constant monomer weight, the total droplet surface area was proportional to $d_{m,i}^{-1}$. However, this was not the case because $d_{m,i}^{-1} \times 10^3$ in decreasing order was SMA (4.0) > LMA (3.7) > PLH (3.2) > PSH (3.0). The reason for this unexpected result is not clear at this point of time.

Although the run with PLH resulted in the largest P_{dye}, the maximum number of monomer droplets that could participate in the particle nucleation process only outnumbered that of the run with PSH (see the $N_{m,i}P_{dye,max}$ data in Table II). Furthermore, the fraction of latex particles generated by monomer droplet nucleation followed the trend SMA > LMA > PSH > PLH (see the $N_{m,i}P_{dye,max}/N_p$ data in Table II). That is, the more hydrophobic the costabilizer was, the stronger the monomer droplet nucleation was. Only 30–40% of the monomer droplets could be successfully converted into latex particles (see the $P_{dye,max}$ data in Table II). In addition, N_p was much larger than the number of particles originating from monomer droplet nucleation ($N_{m,i}P_{dye,max}$), which we attributed to the formation of particle nuclei in the aqueous phase. Latex particles nucleated in the aqueous phase competed effectively with monomer droplets for the incoming radicals, thereby leading to a reduced monomer droplet nucleation. The use of $N_{m,i}P_{dye,max}/N_p$ to discuss the competitive particle nucleation mechanism, should be regarded as qualitative only. This is because $N_{m,i}$ was estimated on the basis of DLS, and this technique resulted in an average hydrodynamic diameter of monomer droplets initially present in the colloidal system ($d_{m,i}$), which was the ratio of the sixth moment to the fifth moment of particle size distribution. Thus, $d_{m,i}$ was larger than the true monomer droplet size. This underestimated $N_{m,i}$ (i.e., the degree of monomer droplet nucleation).

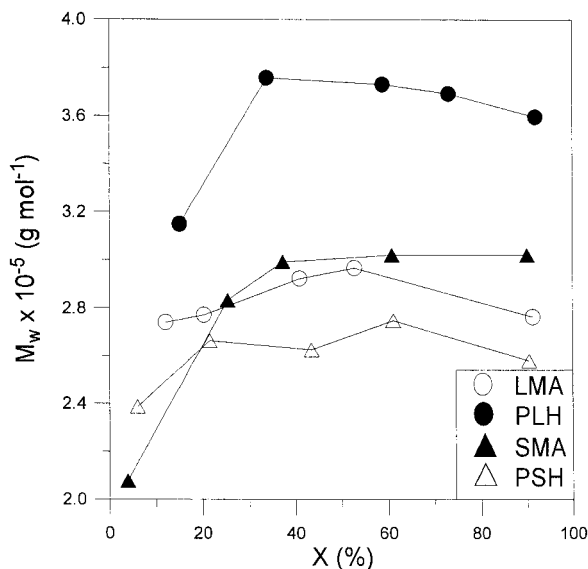Miller et al.[32] showed that monomer droplets were nucleated continuously in the conversion range 0 to

Figure 9 M_w of the polymer at various levels of X in the ST miniemulsion polymerizations with different costabilizers: [SLS] = 10 mM; costabilizer concentration = 3.5 mM; (▲) PSH, (●) PLH, (△) SMA, and (○) LMA.

40–60%. In this study, the conversion at which $P_{dye,max}$ was achieved, in decreasing order, was LMA (43%) > SMA (41%) > PSH (37%) > PLH (34%) (Fig. 8). The formation of particle nuclei in the aqueous phase generated extra particle surfaces, which competed with monomer droplets for the incoming radicals. Under the circumstances, the conversion at which monomer droplet nucleation diminished shifted toward a lower level in comparison with that of the literature.[32] In addition, the stronger the homogeneous nucleation was, the larger the degree of shift in X corresponding to $P_{dye,max}$ was.

Figure 9 shows that particle nucleation diminished and M_w remained relatively constant when X was greater than about 30%. The M_w values in decreasing order were PLH > PSH > LMA > SMA. In emulsion polymerization, the number-average degree of polymerization (X_n) is equal to the rate of growth of a polymeric radical divided by the rate at which the oligomeric radical penetrates the latex particle:[33]

$$X_n = k_p[M]_p N_p / \rho_i \qquad (4)$$

where ρ_i is the rate of generation of initiator radicals in the aqueous phase. X_n is very close to the average kinetic chain length because the termination reaction in the particle involves a polymeric radical and an incoming oligomeric radical. The oligomeric radical has an insignificant influence on the size of the dead polymer chain. The parameters k_p and ρ_i were kept constant in this study. If it was assumed that the difference in $[M]_p$ was insignificant for polymerizations with different costabilizers, M_w should have been proportional to N_p. The N_p values in decreasing

order were PLH > PSH > SMA > LMA, which was quite consistent with the trend of the M_w data. A common feature of the M_w versus X profiles was that M_w first increased and then leveled off with the progress of polymerization. During the early stage of polymerization, the increased M_w with X was most likely due to the increase in N_p (Fig. 7). Figure 9 also shows that polymerizations with PSH, SMA, and LMA showed relatively comparable M_w versus X data. By contrast, the M_w versus X curve of the PLH-containing polymerization deviated significantly from those of the PSH-, SMA-, and LMA-containing polymerizations. A similar phenomenon was also observed in the P_{dye} versus X profiles (Fig. 8).

At the levels of surfactant and polymeric costabilizers investigated in this study, significant Ostwald ripening and homogeneous nucleation made the role of nucleation in homogenized ST emulsion droplets less important. The fact that PSH was more effective as a costabilizer in the ST miniemulsion polymerization compared to PLH implied that the effect of the hydrophobicity outweighed the effect of the degree of polymerization of costabilizer because these two effects are opposite in nature. To improve the effectiveness of this type of comb-like polymeric costabilizers, research on the effects of the concentrations of surfactant and polymeric costabilizer, the number of monomeric units of SMA (or LMA) per chain (i.e., the degree of polymerization), and the hydrophobicity of the backbone of the polymeric costabilizer on the ST miniemulsion polymerization is in progress in our laboratory.

CONCLUSIONS

The polymeric costabilizers PSH and PLH, which are composed of a hydrophilic backbone and several hydrophobic alkyl (stearyl or lauryl) side chains, were prepared and evaluated in the polymerization of homogenized ST emulsions. The hydrophobicity in increasing order was PLH < PSH < LMA < SMA. The more hydrophobic the costabilizer was, the more effective the costabilizer was in retarding Ostwald ripening. The colloidal stability of the homogenized ST emulsion with a very low level (3.5 mM) of PSH or PLH was sufficient to allow monomer droplet nucleation to take place.

The polymerization kinetics were primarily controlled by the hydrophobicity of the costabilizer. The rate of polymerization of the PLH- or PSH-containing polymerization was faster than that of the LMA or SMA counterpart. This was closely related to the number of reaction loci available for the propagation reaction of radicals with the monomer. Only a small fraction of monomer droplets (30–40%) were successfully converted into latex particles. The more hydrophobic the costabilizer was, the stronger the monomer droplet nucleation was. The total number of latex particles was much larger than the number of particles originating from monomer droplet nu-

cleation. This was attributed to the formation of particle nuclei in the aqueous phase. Latex particles nucleated in the aqueous phase exhibited an extremely large particle surface area and, hence, competed effectively with monomer droplets for the incoming radicals. This would suppress the extent of nucleation in monomer droplets.

References

1. Chern, C. S. In Encyclopedia of Surface and Colloid Science; Hubbard, A., Ed.; Marcel Dekker: New York, 2002; p 4220.
2. Ugelstad, J.; El-Aasser, M. S.; Vanderhoff, J. W. J Polym Sci Polym Lett Ed 1973, 11, 503.
3. Capek, I.; Chern, C. S. Adv Polym Sci 2001, 155, 101.
4. Choi, Y. T.; El-Aasser, M. S.; Sudol, E. D.; Vanderhoff, J. W. J Polym Sci Polym Chem Ed 1985, 23, 2973.
5. Rodriguez, V. S.; Delgado, J.; Silebi, C. A.; El-Aasser, M. S. Ind Eng Chem Res 1989, 28, 65.
6. Wang, S.; Schork, F. J. J Appl Polym Sci 1994, 54, 2164.
7. Reimers, J. L.; Skelland, A. H. P.; Schork, F. J. Polym React Eng 1995, 3, 235.
8. Reimers, J. L.; Schork, F. J. J Appl Polym Sci 1996, 59, 1833.
9. Reimers, J. L.; Schork, F. J. J Appl Polym Sci 1996, 60, 251.
10. Wang, S.; Schork, F. J.; Poehlein, G. W.; Gooch, J. W. J Appl Polym Sci 1996, 60, 2069.
11. Blythe, P. J.; Klein, A.; Sudol, E. D.; El-Aasser, M. S. Macromolecules 1999, 32, 6952.
12. Miller, C. M.; Blythe, P. J.; Sudol, E. D.; Silebi, C. A.; El-Aasser, M. S. J Polym Sci Part A: Polym Chem 1994, 32, 2365.
13. Miller, C. M.; Sudol, E. D.; Silebi, C. A.; El-Aasser, M. S. Macromolecules 1995, 28, 2754.
14. Miller, C. M.; Sudol, E. D.; Silebi, C. A.; El-Aasser, M. S. Macromolecules 1995, 28, 2765.
15. Miller, C. M.; Sudol, E. D.; Silebi, C. A.; El-Aasser, M. S. Macromolecules 1995, 28, 2772.
16. Blythe, P. J.; Morrison, B. R.; Mathauer, K. A.; Sudol, E. D.; El-Aasser, M. S. Macromolecules 1999, 32, 6944.
17. Blythe, P. J.; Klein, A.; Sudol, E. D.; El-Aasser, M. S. Macromolecules 1999, 32, 4225.
18. Chern, C. S.; Chen, T. J. Colloid Polym Sci 1997, 275, 546.
19. Chern, C. S.; Chen, T. J. Colloid Polym Sci 1997, 275, 1060.
20. Chern, C. S.; Liou, Y. C.; Chen, T. J. Macromol Chem Phys 1998, 199, 1315.
21. Chern, C. S.; Tang, H. J. Polym React Eng 2003, 11, 213.
22. Chern, C. S.; Chen, T. J. Colloids Surf A 1998, 138, 65.
23. Chern, C. S.; Chen, T. J.; Liou, Y. C. Polymer 1998, 39, 3767.
24. Rehfeld, S. J. J Phys Chem 1967, 71, 738.
25. Sutterlin, N. In Polymer Colloids; Fitch, R. M., Ed.; Plenum: New York, 1980; p Vol. II, 583.
26. Properties of Polymers: Their Correlation with Chemical Structure; Their Numerical Estimation and Prediction from Additive Group Contributions, 3rd ed: van Krevelen, D. W., Ed.; Elsevier: London, 1997.
27. Kabalnov, A. S.; Shchukin, E. D. Adv Colloid Interface Sci 1992, 38, 69.
28. Ugelstad, J.; Mork, P. C.; Kaggerud, K. H.; Ellingsen, T.; Berge, A. Adv Colloid Interface Sci 1980, 13, 101.
29. Davies, J. T. Turbulence Phenomena; Academic: New York, 1972.
30. Gilbert, R. G. Pure Appl Chem 1996, 68, 1491.
31. Chang, H. C.; Lin, Y. Y.; Chern, C. S.; Lin, S. Y. Langmuir 1998, 14, 6632.
32. Miller, C. M.; Sudol, E. D.; Silebi, C. A.; El-Aasser, M. S. J Polym Sci Polym Chem 1995, 33, 1391.
33. Eliseeva, V. I.; Ivanchev, S. S.; Kuchanov, S. I.; Lebedev, A. V. Emulsion Polymerization and its Applications in Industry; Consultants Bureau: New York, 1981.